Immunology
The Journal of cells, molecules, systems and technologies

British Society for immunology

IMMUNOLOGY ORIGINAL ARTICLE

Interleukin-22 and CD160 play additive roles in the host mucosal response to *Clostridium difficile* infection in mice

Amir A. Sadighi Akha,[1] Andrew J. McDermott,[2] Casey M. Theriot,[3] Paul E. Carlson Jr,[2] Charles R. Frank,[1] Roderick A. McDonald,[1] Nicole R. Falkowski,[1] Ingrid L. Bergin,[4] Vincent B. Young[2,3] and Gary B. Huffnagle[1,2]

[1]*Division of Pulmonary and Critical Care Medicine, Department of Internal Medicine, University of Michigan Medical School, Ann Arbor, MI,* [2]*Department of Microbiology and Immunology, University of Michigan Medical School, Ann Arbor, MI,* [3]*Division of Infectious Diseases, Department of Internal Medicine, University of Michigan Medical School, Ann Arbor, MI, and* [4]*Unit for Laboratory Animal Medicine, University of Michigan Medical School, Ann Arbor, MI, USA*

doi:10.1111/imm.12414
Received 13 August 2014; revised 6 October 2014; accepted 13 October 2014.
Correspondence: Dr Amir A. Sadighi Akha, Division of Clinical Biochemistry and Immunology, Department of Laboratory Medicine and Pathology, Mayo Clinic, Rochester, MN 55905, USA.
E-mail: sadighiakha.amir@mayo.edu
Senior author: Dr Gary B. Huffnagle
E-mail: ghuff@umich.edu

Summary

Our previous work has shown the significant up-regulation of *Il22* and increased phosphorylation of signal transducer and activator of transcription 3 (STAT3) as part of the mucosal inflammatory response to *Clostridium difficile* infection in mice. Others have shown that phosphorylation of STAT3 at mucosal surfaces includes interleukin-22 (IL-22) and CD160-mediated components. The current study sought to determine the potential role(s) of IL-22 and/or CD160 in the mucosal response to *C. difficile* infection. *Clostridium difficile*-infected mice treated with anti-IL-22, anti-CD160 or a combination of the two showed significantly reduced STAT3 phosphorylation in comparison to *C. difficile*-infected mice that had not received either antibody. In addition, *C. difficile*-infected mice treated with anti-IL-22/CD160 induced a smaller set of genes, and at significantly lower levels than the untreated *C. difficile*-infected mice. The affected genes included pro-inflammatory chemokines and cytokines, and anti-microbial peptides. Furthermore, histopathological and flow cytometric assessments both showed a significantly reduced influx of neutrophils in *C. difficile*-infected mice treated with anti-IL-22/CD160. These data demonstrate that IL-22 and CD160 are together responsible for a significant fraction of the colonic STAT3 phosphorylation in *C. difficile* infection. They also underscore the additive effects of IL-22 and CD160 in mediating both the pro-inflammatory and pro-survival aspects of the host mucosal response in this infection.

Keywords: *Clostridium difficile*; CD160; interleukin-22; pSTAT3; RegIIIγ.

Introduction

Clostridium difficile is a Gram-positive, spore-forming, anaerobic bacterium.[1] It is the most prevalent cause of nosocomial infectious diarrhoea in antibiotic-treated patients.[2–5] In antibiotic-treated individuals, *C. difficile* spores can germinate, replicate as vegetative bacteria and produce exotoxins, particularly TcdA and TcdB, which act as the bacterium's main virulence factors. Both TcdA and TcdB are glucosyltransferases that irreversibly inactivate small GTPases of the Rho family.[6,7] As a result, the epithelial actin cytoskeleton is depolymerized, the function of tight junctions is impaired, and severe epithelial cell damage ensues.[8–10] Infection with *C. difficile* can lead to a broad range of clinical outcomes, including asymptomatic colonization, mild diarrhoea, severe pseudomembranous colitis and toxic megacolon.[2,11]

In recent years, a number of groups have used an approach in which mice are treated with antibiotics prior to oral challenge with *C. difficile* to study the host response to *C. difficile* infection. These studies have proven the higher susceptibility of MyD88$^{-/-}$,[12] TLR4$^{-/-}$,[13] NOD1$^{-/-}$[14] and ASC$^{-/-}$[15] mice to *C. difficile* infection, and the protective effect of TLR5 stimulation against acute *C. difficile* colitis.[16] Based on the findings in MyD88$^{-/-}$, NOD1$^{-/-}$ and ASC$^{-/-}$ mice, it is now believed that NOD1, MyD88 and interleukin-1β (IL-1β) signalling enhance the expression of CXCL1 in the colon in *C. difficile*-infected mice, thereby inducing neutrophil influx to the site of infection.[17]

Recent work from our laboratory has shown that acute infection of mice with *C. difficile* leads to pro-survival signalling as part of the mucosal inflammatory response.[18] The infected mice display a significant up-regulation in the expression of chemokines (including *Cxcl1*, *Cxcl2* and

Ccl2), numerous pro-inflammatory cytokines (including *Ifng*, *Il1b*, *Il6* and *Il17f*), as well as *Il22* and a number of anti-microbial peptides (including *Defa1*, *Defa28*, *Defb1*, *Slpi* and *Reg3g*). In addition, they show significantly higher phosphorylation of eukaryotic initiation factor 2α (eIF2α) and signal transducer and activator of transcription 3 (STAT3) in their caeca and colons. These data prompted us to speculate that either eIF2α phosphorylation or the IL-22-pSTAT3-RegIIIγ axis could potentially be used to affect the nature of the host mucosal response to *C. difficile* infection.

The herpes virus entry mediator (HVEM), the first recognized entry route for herpes simplex virus (HSV), is a cell surface molecule from the tumour necrosis factor receptor superfamily.[19] HVEM has been identified as a colitis risk locus in humans,[20] and plays a dual role in the development of colitis in the mouse model.[21,22] So far, as a receptor, HVEM has been shown to bind five ligands: the HSV envelope glycoprotein-D (gD)[23]; the tumour necrosis factor-related cytokines LIGHT and lymphotoxin-α;[24] and the immunoglobulin superfamily members B and T lymphocyte attenuator (BTLA)[25] and CD160.[26] gD, BTLA and CD160 bind HVEM through a binding site (CRD1) that is distinct from the one for LIGHT (CRD2).[27] Depending on the ligand it binds, the cell types involved and the context of engagement, HVEM can activate co-stimulatory or co-inhibitory signalling pathways.[28–30] The balance of the pro-inflammatory and anti-inflammatory effects of HVEM signalling in a specific case is the result of the interplay of HVEM interactions with its various ligands on cells of both the innate and adaptive immune systems.[21] A more recent report has focused on the role of HVEM in mucosal defence against pathogenic bacteria.[31] It shows the contribution of HVEM to host defence against *Citrobacter rodentium* infection in the gut and *Streptococcus pneumoniae* infection in the lung. More specifically, it provides evidence that phosphorylation of STAT3 in mucosal epithelial cells includes IL-22- and CD160-mediated components and stipulates that HVEM signalling, through its ligand CD160, acts cooperatively with IL-22 signalling to induce optimal STAT3 activation for host defence at mucosal barriers.[31]

Based on our findings on the host response to *C. difficile* infection,[18] and the recent report on the role of HVEM/CD160 in host defence at mucosal barriers,[31] we devised the current study to examine the effects of IL-22 and CD160, and their potential interaction, on the mouse mucosal response to *C. difficile* infection.

Materials and methods

Ethics statement

All animal experiments were conducted with the approval of the University Committee on Use and Care of Animals (UCUCA) at the University of Michigan. The University's animal care policies follow the Public Health Service policy on Humane Care and Use of Laboratory Animals. The mice were housed in an AAALAC-accredited facility. None of the conducted experiments involved the deliberate induction of discomfort or injury. The physical condition and behaviour of the mice were assessed on a daily basis. The mice were euthanized by CO_2 asphyxiation in compliance with the recommendations of the Panel on Euthanasia of the American Veterinary Medical Association.

Animals

Wild-type C57BL/6 mice obtained from Jackson Laboratories (Bar Harbor, ME) were used to establish a breeding colony at the University of Michigan Medical School. They were housed under specific pathogen-free conditions and consumed clean food and water *ad libitum*. Male mice at 5–8 weeks of age were used for the current set of experiments.

Bacterial growth conditions and spore preparations

Clostridium difficile strain 630 (ATCC 1382) was cultured in an anaerobic chamber (Coy Laboratory Products, Grass Lake Charter Township, MI). For routine growth and maintenance, the isolates were cultured on brain–heart infusion broth supplemented with 0·5% yeast extract and 0·1% cysteine (BHIS) plates. Spore stocks for *C. difficile* 630 were produced as follows: An early spore preparation was used to reconstitute vegetative cells by plating on BHIS + 0·1% taurocholate. An isolated colony was used to inoculate an overnight culture of Columbia broth. Two millilitres of the overnight culture was then used to inoculate 40 ml of Clospore medium,[32] upon which the culture was allowed to grow for 7 days. Cultures were then washed at least four times in cold water to remove vegetative cell debris. Spore stocks were stored in water at 4° until use.

Antibodies

Antibodies against IL-22 (clone IL22JOP) and CD160 (clone CNX46-3) were purchased from eBioScience (San Diego, CA). The conjugated antibodies used for flow cytometry, including the ones against CD11b (clone M1/70), CD11c (clone HL3), CD45 (clone 30-F11), Ly6C (clone AL-21) and Ly6G (clone 1A8), as well as an unconjugated antibody against FcRIII/II (clone 2.4G2), were purchased from BD Biosciences (San Diego, CA) and Biolegend (San Diego, CA). Those against phospho-STAT3 (clone D3A7) and STAT3 (clone 79D7) were obtained from Cell Signaling Technology (Danvers, MA). Alkaline phosphatase-conjugated anti-rabbit antibody was from Santa Cruz Biotechnology (Santa Cruz, CA).

Administration of antibiotics, infecting mice with C. difficile 630 and antibody treatment

5- to 8-week-old male wild-type C57BL/6 mice were either left untreated (defined as untreated mice) or received cephoperazone (0·5 g/l) in sterile drinking water for 5 days. The mice receiving the antibiotic were then switched to regular drinking water for 2 days. Afterwards, each of the mice that had received cephoperazone was given 10^6 spores of the *C. difficile* 630 strain by oral gavage.[33] It should be noted that we had used the VPI 10463 strain to infect mice in our previous report.[18] The decision to change the strain in the current study was based on the finding that the 630 strain leads to a less severe and more prolonged course of infection,[33] and therefore could potentially provide broader latitude for a given treatment to affect the outcome. The *C. difficile*-infected mice consisted of four subgroups: the first received neither anti-IL-22 nor anti-CD160 (CDI); the second received anti-IL-22 (CDI + anti-IL-22); the third received anti-CD160 (CDI + anti-CD160); and the fourth received both anti-IL-22 and anti-CD160 (CDI + anti-IL-22/CD160). The mice received the antibodies by intraperitoneal injection on days – 1, 1, 2 and 3. Each mouse received 100 μg of the relevant antibody(ies) on each occasion. All the animals were monitored for signs of disease including diarrhoea, hunched posture and weight loss. All the mice were killed 96 hr after the infection (Fig. 1).

Assessment of C. difficile colonization

A species-specific quantitative PCR was used to determine *C. difficile* colonization in colon snips collected at the time of necropsy. DNA extraction and *C. difficile* species-specific quantitative PCR were performed as described previously.[34,35] Raw C_t values were normalized to a single copy per genome host gene to generate ΔC_t values.[34–36] ΔC_t values were then converted to 'detectable genomes/g host tissue' using a standard curve generated with known amounts of vegetative *C. difficile* and colonic tissue. The analytic limit of detection of the assay is ~ 10^3 genomes/g of host tissue.

Enrichment of colonic leucocytes

Colonic leucocyte enrichment was performed as previously described,[18] with certain modifications. The colon of each mouse was excised, opened longitudinally and washed in PBS to remove the faecal content. Afterwards, each colon was incubated in calcium- and magnesium-free Hanks' balanced salt solution (HBSS) containing 2·5% fetal bovine serum, 1 mM dithiothreitol (DTT) and 5 mM EDTA for 20 min at 37°, washed and then incubated in calcium- and magnesium-free HBSS containing 2·5% fetal bovine serum, 400 U/ml collagenase type 3 (Worthington Biochemical, Freehold, NJ) and 0·5 mg/ml DNase I (Roche, Indianapolis, IN) for 60 min at 37°. The digested samples were re-suspended in a 20% Percoll solution (Sigma Aldrich, Milwaukee, WI) and centrifuged at 900 ***g*** for 30 min at room temperature. The resulting pellet was then washed and re-suspended in staining buffer (HBSS containing 0·5% BSA and 0·1% sodium azide).

Flow cytometry

Cell suspensions prepared from colonic digests were stained for flow cytometric analysis as previously described.[18] Briefly, colonic digests re-suspended in staining buffer were pre-blocked with unlabelled anti-FcRIII/II

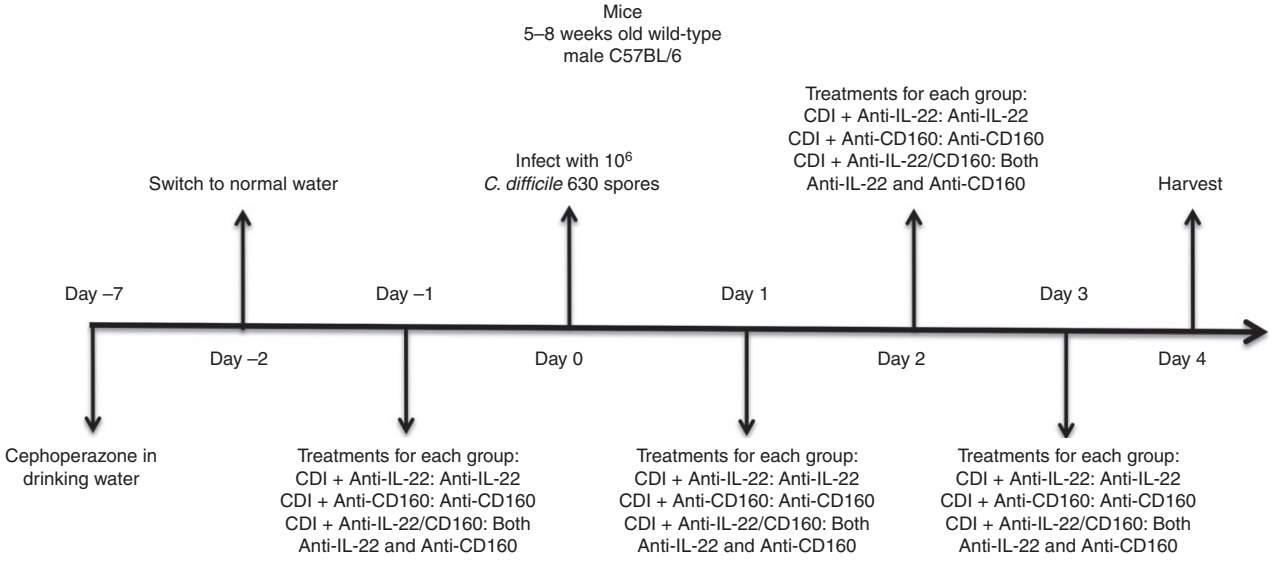

Figure 1. Experimental timeline of the *Clostridium difficile* 630 infection.

antibody. Afterwards, the cells were stained in a final volume of 100 µl in 96-well round bottom plates for 30 min. The cells were then washed (×2) in the staining buffer and re-suspended in BD Biosciences' stabilizing fixative. Data on the samples were acquired on a 3-laser Canto II flow cytometer using FACSDIVA software (BD Biosciences). The acquired data were analysed with the FLOWJO software (TreeStar, Ashland, OR). Leucocytes were defined as cells with surface expression of CD45. Neutrophils were identified within this population by first gating on the $CD11b^{high}$ $CD11c^{low}$ cells, followed by gating on $Ly6C^{high}$ events. The $Ly6G^{high}$ cells within the $Ly6C^{high}$ population were defined as neutrophils.

Histopathology

Colonic tissue from each mouse was placed in a histology cassette and fixed with 10% neutral buffered formalin for 24 hr and then transferred to 70% ethyl alcohol. The cassettes were then paraffin-embedded, sectioned and stained with haematoxylin & eosin for histopathological evaluation (McClinchey Histology Lab, Stockbridge, MI). Slides were examined on an Olympus BX45 light microscope (Olympus Corporation, Center Valley, PA), and were scored by a board-certified veterinary pathologist blinded to the experimental set-up. Neutrophilic inflammation was assessed semi-quantitatively according to a previously published scoring system.[37] Briefly, neutrophilic inflammation scores were graded as follows: (0) no inflammation; (1) minimal multifocal neutrophilic inflammation (marginating or perivascular neutrophils in submucosa, minimal intraepithelial and proprial neutrophils); (2) moderate multifocal neutrophilic inflammation (perivascular and interstitial neutrophils in submucosa, mild to moderate intraepithelial and proprial neutrophils); (3) severe multifocal to coalescing neutrophilic inflammation (perivascular and increased interstitial neutrophils in submucosa with or without extension to muscular wall, moderate intraepithelial neutrophils); and (4) same as score 3 with abscesses.

Representative images were taken with a QImaging MicroPublisher RTV 5.0 camera (QImaging Corporation, Surrey, BC), at ×100 and ×400 magnifications. Images were acquired using QCAPTURE SUITE PLUS (QImaging Corporation). Image processing and composite construction were performed in ADOBE PHOTOSHOP (San Jose, CA). Image processing was limited to global adjustments of brightness, contrast, exposure, sharpness, image size and colour balance as needed.

Western blot analysis

Immunoblotting was performed as previously described.[18] Briefly, colon snips obtained from untreated mice and the ones in each of the other experimental groups were homogenized on ice with a rotor/stator-type homogenizer (Biospec Products, Bartlesville, OK) while immersed in ice-cold modified RIPA buffer supplemented with HALT protease and phosphatase inhibitor cocktail (Thermo Fisher, Rockford, IL). All tissue lysates were subjected to two rounds of centrifugation at 10 000 ***g*** for 10 min. The bicinchoninc acid protein assay (Thermo Fisher) was used to determine the protein concentration of each of the cleared lysates. Thirty micrograms of each colon lysate protein was boiled for 5 min in reducing sample buffer containing DTT and resolved by SDS–PAGE electrophoresis, transferred to PVDF membranes and probed with the indicated antibodies. The membranes were exposed to enhanced chemifluorescence substrate (GE Healthcare, Piscataway, NJ), followed by scanning on a Typhoon $Trio^{+}$ imaging system (GE Healthcare) to obtain a digital image of the probed protein. The bands were then quantified with IMAGEQUANT software (GE Healthcare).

Quantification of mRNA levels using custom-made quantitative RT-PCR cards

Quantification of mRNA levels was performed as previously described.[18] Briefly, colon snips obtained from untreated mice and the ones in each of the other experimental groups were homogenized with a rotor/stator-type homogenizer while immersed in TRIzol RNA reagent (Life Technologies, Grand Island, NY). The TRIzol RNA reagent and the RNeasy Mini kit (Qiagen, Valencia, CA) were used in successive steps to isolate RNA from the colon samples, each according to its manufacturer's instructions. An Agilent Bioanalyser (Agilent Technologies, Palo Alto, CA) and a Nanodrop instrument (Thermo Fisher) were used to determine the quality and concentration of each RNA isolate respectively. Complementary DNA (cDNA) was generated from each RNA sample using the RT^2 First Strand kit (Qiagen). Expression levels of the genes under study were determined by using a set of mouse RT^2 Profiler PCR cards (Qiagen), custom-made to contain eight replicate sets of 48 primer pairs (Table 1). Each well of the replicate sets was loaded with 5 ng of cDNA reaction product. Each card was run on a LightCycler 480 real-time PCR system (Roche). The relative RNA expression levels were inferred from the C_t values.

Statistical analyses

For the *C. difficile* colonization assay, the difference between the untreated mice with the CDI, the CDI + anti-IL-22, the CDI + anti-CD160, and the CDI + anti-IL-22/CD160 groups of *C. difficile*-infected mice was evaluated

Table 1. List of evaluated genes. The groupings of the genes is based on either the structural relationship of the particular set of genes, and/or on their established (or purported) functions

Chemokines	*Ccl2*	*Ccl3*	*Ccl4*	*Cxcl1*	*Cxcl2*	*Cxcl9*	*Cxcl10*		
Cytokines and related molecules	*Il1b*	*Il4*	*Il6*	*Il10*	*Il12a*	*Il13*	*Il17a*	*Il17f*	
	Il22	*Il23a*	*Il25*	*Ifng*	*Tgfb1*	*Tnfa*	*Tslp*		
Anti-microbial peptides	*Camp*	*Defa1*	*Defa4*	*Defb1*	*Defb3*	*Reg3g*	*Slpi*		
Nod-like receptors	*Nod1*	*Nod2*							
Short-chain fatty acid receptors	*Ffar2*	*Ffar3*	*Gpr35*						
Tight junction and adhesion proteins	*Cldn1*	*Cldn2*	*Epcam*	*Tjp1*	*Tjp2*				
Miscellaneous	*Actb*	*Arg1*	*Gapdh*	*Hgf*	*Mgdc*	*Mpo*	*Nos2*	*Retnla*	*Shh*

for significance by using the Kruskal–Wallis test followed by Dunn's multiple comparisons test with significance set at $P \leq 0{\cdot}05$. For both STAT3 phosphorylation, and scoring of neutrophilic inflammation, the difference between the untreated mice with the CDI, the CDI + anti-IL-22, the CDI + anti-CD160, and the CDI + anti-IL-22/CD160 groups of *C. difficile*-infected mice was evaluated for significance by using one-way analysis of variance with Geisser–Greenhouse correction followed by Fisher's least significant difference test with significance set at $P \leq 0{\cdot}05$.

The quantitative RT-PCR data acquired with custom-made cards were normalized as previously described.[18,38] The normalized numbers were used to calculate ΔC_t values for each gene by deducting the geometric mean of the *Actb* and *Gapdh* C_t values of each sample from the C_t value of each gene in that sample.[39] The SAM (Statistical Analysis for Microarray) software developed by Tusher and colleagues[40] was then used to compare the expression levels of each gene between the colons of different groups of mice. In each case, genes for which false discovery rate $\leq 0{\cdot}05$ were considered significant.[41] All the significant genes with at least a twofold change in expression were defined as up- (or down)-regulated.

Results

C. difficile 630 colonizes mice pre-treated with cephoperazone

The timeline and details of the experiment, as described in the Materials and methods section, are depicted in Fig. 1. Following pre-treatment with cephoperazone, the mice received an oral gavage of 10^6 spores of *C. difficile* strain 630 on day 0. All the *C. difficile*-infected mice showed a gradual decline in weight over the course of infection (Fig. 2a). A *C. difficile*-specific quantitative PCR assay showed the significant colonization of the colons of all the *C. difficile*-infected mice with *C. difficile* at the end of the experimental period, i.e. day 4 of infection (Fig. 2b). There was no significant difference in *C. difficile* load between *C. difficile*-infected mice that had not received either anti-IL-22 or anti-CD160 (CDI), *C.*

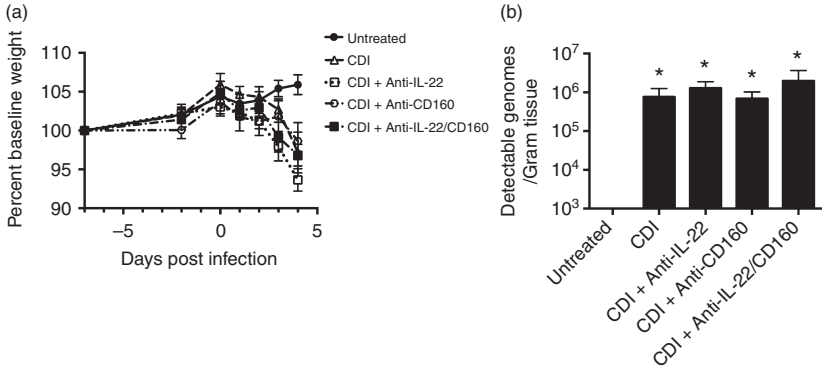

Figure 2. Reduction in weight of *Clostridium difficile*-infected mice, and significant colonization of their colons with *C. difficile*. (a) Reduction in weight of *C. difficile*-infected mice in comparison to their untreated counterparts ($n = 8$ for each group) from two sets of experiments. (b) A species-specific quantitative PCR assay was used to quantify *C. difficile* colonization in the colons ($n = 8$ in each group) of untreated mice, *C. difficile*-infected mice that had not received either anti-interleukin-22 (IL-22) or anti-CD160 (CDI), CDI + anti-IL-22 mice, CDI + anti-CD160 mice, and CDI + anti-IL-22/CD160 mice from two sets of experiments. Each bar represents the mean ± SEM of the *C. difficile* load. ★ denotes a significant difference in colonization with the untreated mice, i.e. a P value of $\leq 0{\cdot}05$ for the Dunn's post hoc test. The analytic limit of detection of the assay is ~ 10^3 genomes/g of host tissue.

difficile-infected mice that had received anti-IL-22 (CDI + anti-IL-22), *C. difficile*-infected mice that had received anti-CD160 (CDI + anti-CD160), and *C. difficile*-infected mice that had received both anti-IL-22 and anti-CD160 (CDI + anti-IL-22/CD160).

Anti-IL-22, anti-CD160 and combined anti-IL-22/CD160 treatment significantly reduce STAT3 phosphorylation in *C. difficile*-infected mice

We have previously shown that *C. difficile* strain VPI 10463 induces phosphorylation of STAT3 in the colons of infected mice.[18] To examine the effect of infection with *C. difficile* 630 on STAT3 phosphorylation levels, colonic protein lysates from untreated mice, CDI mice, CDI + anti-IL-22 mice, CDI + anti-CD160 mice, and CDI + anti-IL-22/CD160 mice were probed for the phosphorylation levels of STAT3. Consistent with our previous findings, colons of CDI mice showed a significant increase in STAT3 phosphorylation in comparison to untreated mice (Fig. 3). CDI + anti-IL-22 mice, CDI + anti-CD160 mice, and CDI + anti-IL-22/CD160 mice also had significantly higher levels of phosphorylated STAT3 than the untreated mice.

We then analysed the effect of antibody treatment on STAT3 phosphorylation in *C. difficile*-infected mice. Based on this analysis, CDI + anti-IL-22 mice, CDI + anti-CD160 mice, and CDI + anti-IL-22/CD160 mice all had significantly lower levels of phosphorylated STAT3 than the CDI mice (Fig. 3).

Combined anti-IL-22/CD160 treatment significantly alters the mucosal gene expression pattern in response to *C. difficile* infection

In our previous study, we had used a quantitative RT-PCR approach to examine the host mucosal response in mice infected with the VPI 10463 strain of *C. difficile*.[18] This had shown a significant increase in the expression of a number of chemokines, pro-inflammatory cytokines, as well as *Il22* and a number of anti-microbial peptides at the sites of infection. We adopted a similar approach in the current work, where we examined the expression patterns of 45 genes (see Table 1) in the colons of mice infected with *C. difficile* 630 (CDI). The infected mice displayed a significant up-regulation of the chemokines *Ccl2*, *Ccl3*, *Ccl4*, *Cxcl1*, *Cxcl2*, *Cxcl9* and *Cxcl10*; the cytokines *Ifng*, *Il1b*, *Il6*, *Tnfa*, *Il12a*, *Il22* and *Il25*; the anti-microbial peptides *Defa1*, *Defb1*, *Reg3g* and *Slpi*; as well as *Arg1*, *Ffar3*, *Mpo* and *Nos2* in comparison to the untreated mice (Fig. 4a); a pattern closely comparable to our previous findings.[18]

Having established that the gene expression pattern in the colons of mice infected with *C. difficile* 630 (CDI) is closely comparable to that of mice infected with *C. difficile* VPI 10463,[18] we proceeded to evaluate the effects of anti-IL-22, anti-CD160 and anti-IL-22/CD160 treatments on the mice infected with *C. difficile* 630 (CDI). To examine the matter closely, we performed a statistical comparison between the genes expressed in the CDI mice and each of the following groups: CDI + anti-IL-22 mice (Fig. 4b), CDI + anti-CD160 mice (Fig. 4c),

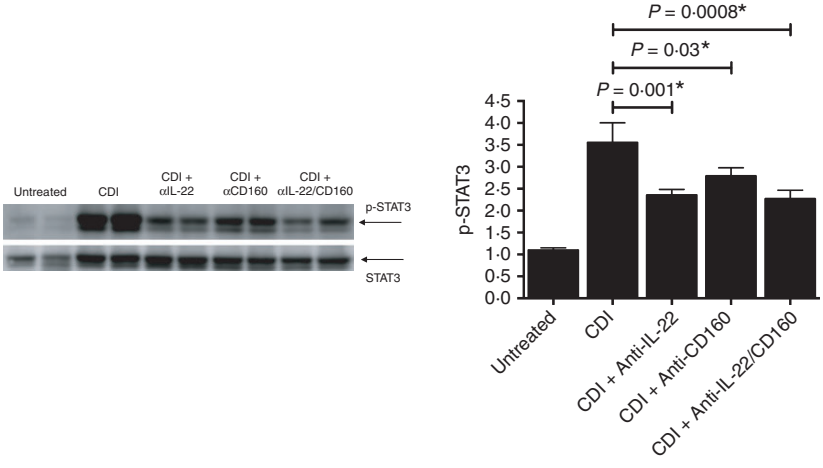

Figure 3. Significant reduction in signal transducer and activator of transcription 3 (STAT3) phosphorylation in *Clostridium difficile*-infected mice treated with anti-interleukin-22 (IL-22), anti-CD160 or anti-IL-22/CD160. Protein lysates from the colons ($n = 8$ in each group) of untreated mice, CDI mice, CDI + anti-IL-22 mice, CDI + anti-CD160 mice, and CDI + anti-IL-22/CD160 mice from two sets of experiments were used to evaluate the phosphorylation of STAT3 by immunoblotting. The panel on the left shows the image of the immunoblot for two colons of each experimental group, and the bar graph on the right depicts the mean ± SEM of the response for all eight colons in each group. A *P*-value of $\leq 0{\cdot}05$ indicates a significant difference in STAT3 phosphorylation with the CDI mice and is marked with a ★. All four groups of *C. difficile*-infected mice had significantly higher STAT3 phosphorylation than their untreated counterparts: CDI ($P < 0{\cdot}0001$), CDI + anti-IL-22 ($P = 0{\cdot}001$), CDI + anti-CD160 ($P < 0{\cdot}0001$), and CDI + anti-IL-22/CD160 ($P = 0{\cdot}001$) (not marked on the figure).

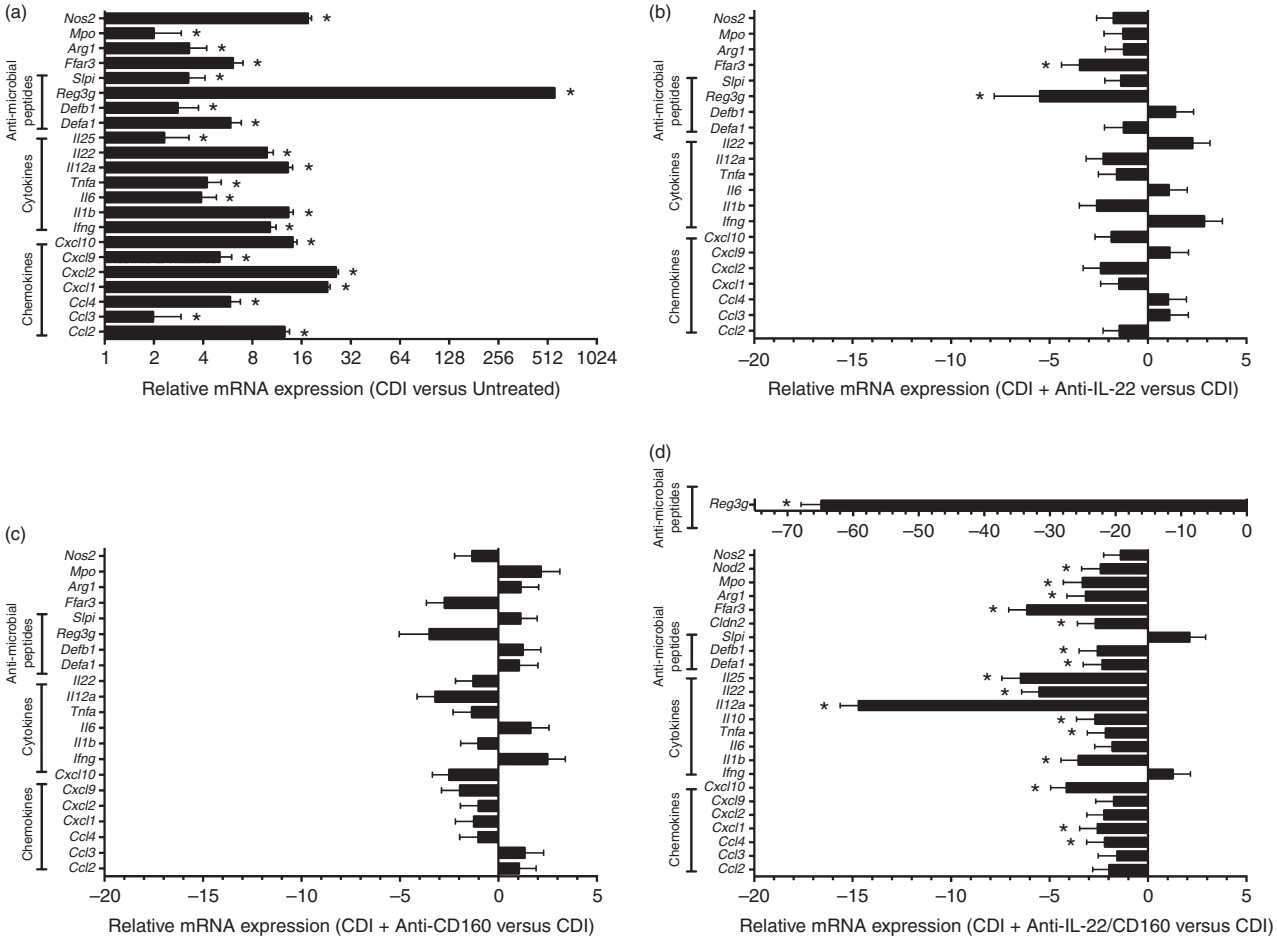

Figure 4. Combined anti-interleukin-22 (IL-22)/CD160 treatment significantly alters the mucosal gene expression pattern in response to *Clostridium difficile* infection. Custom-made RT-PCR cards were used to evaluate gene expression levels in the colons (n = 5 in each group) of untreated mice, CDI mice, CDI + anti-IL-22 mice, CDI + anti-CD160 mice, and CDI + anti-IL-22/CD160 mice from two sets of experiments. The panel on the top left shows the significantly up-regulated genes in the colons of CDI mice in comparison to untreated mice (a). The remaining panels show the change in expression of the genes depicted in (a) in CDI + anti-IL-22 mice (b); CDI + anti-CD160 mice (c); and CDI + anti-IL-22/CD160 mice (d), as compared to CDI mice respectively (d also depicts *Nod2*, *Cldn2* and *Il10*, which have significantly different expression levels between CDI and CDI + anti-IL-22/CD160 mice but not between CDI and untreated mice). Each bar represents the mean ± SEM of the relative expression of the depicted gene. In each panel, ★ denotes a significant difference in expression levels between the specified groups of mice, i.e. false discovery rate $\leq 0{\cdot}05$. It should be noted that a $\log_2$ scale is used for the graphs in (a), whereas the graphs in (b), (c) and (d) are on a linear scale. Due to the intensity of its down-regulation, the *Reg3g* result in (d) is graphed separately.

and CDI + anti-IL-22/CD160 mice (Fig. 4d). Based on these analyses, in CDI + anti-IL-22 mice, only two genes were expressed at significantly lower levels than the CDI mice; *Reg3g* (about fivefold less) and *Ffar3* (about twofold less) (Fig. 4b). Furthermore, there was no significant difference in gene expression between the CDI mice and the CDI + anti-CD160 mice (Fig. 4c). By contrast, CDI + anti-IL-22/CD160 mice had a significant reduction in the expression levels of 17 genes in comparison to the CDI mice (Fig. 4d). These included the chemokines *Ccl4*, *Cxcl1* and *Cxcl10*; the cytokines *Il1b*, *Tnfa*, *Il10*, *Il12a*, *Il22* and *Il25*; the anti-microbial peptides *Defa1*, *Defb1* and *Reg3g*; as well as *Arg1*, *Cldn2*, *Ffar3*, *Mpo* and *Nod2*.

Combined anti-IL-22/CD160 treatment reduces neutrophil infiltration in response to *C. difficile* infection

The decreased expression of *Cxcl1*, which plays a well-documented role in neutrophil influx to the colons of *C. difficile*-infected mice, and *Mpo* (Fig. 4d) in the colons of CDI + anti-IL-22/CD160 mice led us to speculate that these mice should have a lower neutrophilic infiltrate at the site of infection than the three other groups of *C. difficile*-infected mice, i.e. CDI mice, CDI + anti-IL-22 mice, and CDI + anti-CD160 mice. This premise was assessed by two different approaches. First, haematoxylin & eosin-stained colonic tissues (Fig. 5a) were scored

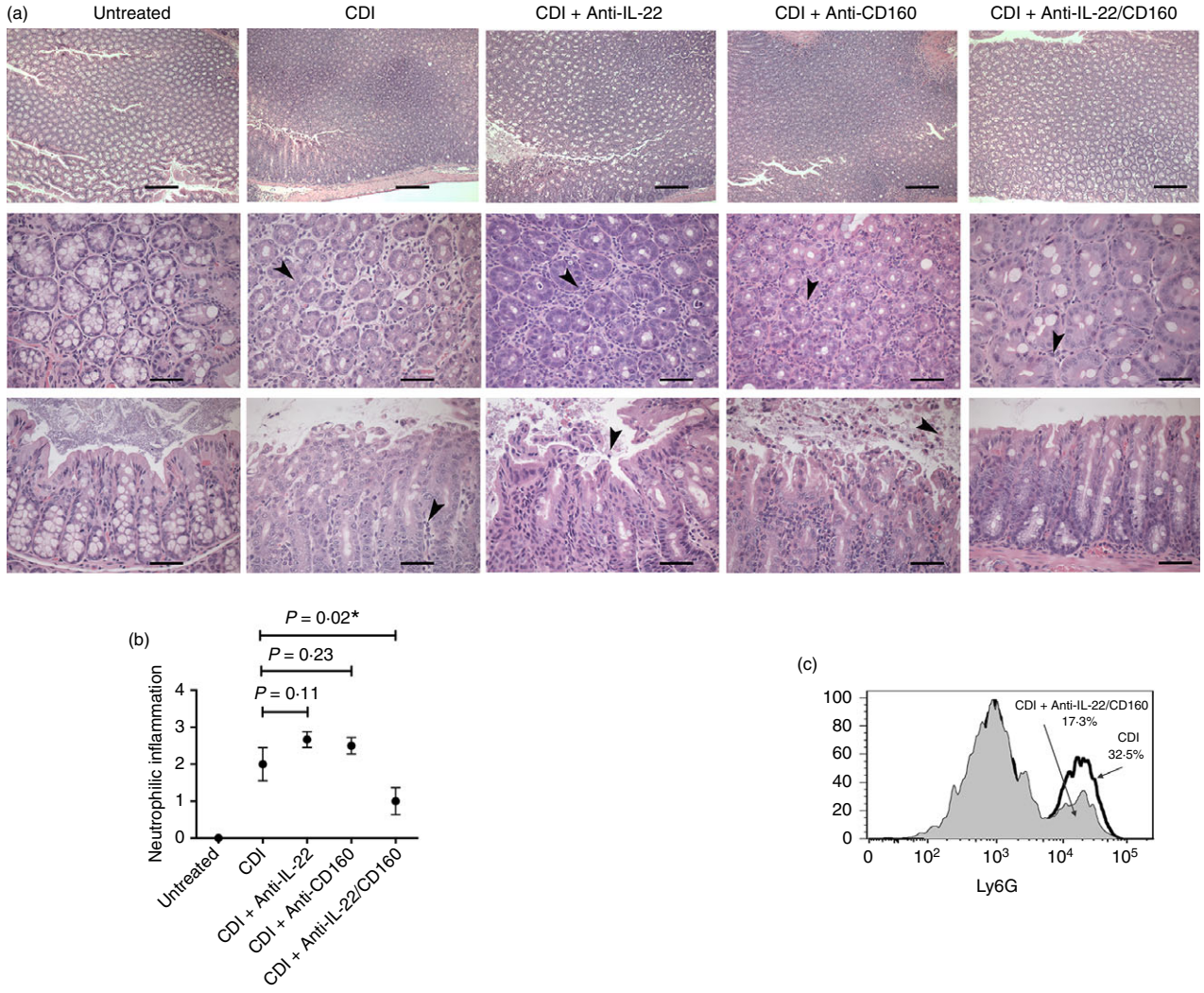

Figure 5. Combined anti-interleukin-22 (IL-22)/CD160 treatment reduces neutrophil infiltration in response to *Clostridium difficile* infection. (a) Representative photomicrographs of haematoxylin & eosin-stained colonic sections from untreated mice, CDI mice, CDI + anti-IL-22 mice, CDI + anti-CD160 mice and CDI + anti-IL-22/CD160 mice. The sections illustrate reduced inflammatory infiltration in the CDI + anti-IL-22/CD160 mice in comparison to the CDI, the CDI + anti-IL-22, and the CDI + anti-CD160 groups of mice. Arrowheads point to cellular infiltrates within each section. The top row of images are at ×100 original magnification, with the bar = 200 μm length. All other images are at ×400 original magnification, with the bar = 50 μm length. (b) Graph depicting the mean ± SEM of the neutrophil infiltration scores for untreated mice, CDI mice, CDI + anti-IL-22 mice, CDI + anti-CD160 mice and CDI + anti-IL-22/CD160 mice ($n = 6$ in each group) from two sets of experiments. A P-value of $\leq 0{\cdot}05$ indicates a significant difference in neutrophil influx score with the CDI mice and is marked with a ★. All four groups of *C. difficile*-infected mice had significantly higher neutrophil influx scores than their untreated counterparts: CDI ($P < 0{\cdot}0001$), CDI + anti-IL-22 ($P < 0{\cdot}0001$), CDI + anti-CD160 ($P < 0{\cdot}0001$), and CDI + anti-IL-22/CD160 ($P = 0{\cdot}02$) (not marked on the figure). The differences between both CDI + anti-IL-22 mice with CDI + anti-IL-22/CD160 ($P = 0{\cdot}005$), and CDI + anti-CD160 mice with CDI + anti-IL-22/CD160 mice ($P = 0.001$) were also significant (not marked on the figure). (c) Decreased influx of neutrophils to the colons of CDI + anti-IL-22/CD160 mice in comparison to CDI mice as assessed by flow cytometry. The histograms are concatenated overlays of three mice from each group.

for neutrophilic inflammation. This showed a significant reduction in neutrophilic infiltrate in CDI + anti-IL-22/CD160 mice in comparison to CDI mice; by contrast, neither CDI + anti-IL-22 mice, nor CDI + anti-CD160 mice showed a significant difference in neutrophil infiltration with CDI mice (Fig. 5b). To complement the scoring outcome, we used flow cytometry to compare the influx of neutrophils into the colons of CDI mice and CDI + anti-IL-22/CD160 mice. As expected, CDI mice showed a substantial influx of $Ly6G^{high}$ cells, i.e. neutrophils, into their colons. The CDI + anti-IL-22/CD160 mice showed a clear reduction in the influx of $Ly6G^{high}$ cells in comparison to the CDI mice (Fig. 5c), thereby confirming the histopathological findings.

Discussion

This study was conducted to examine the effects of IL-22 and CD160, and their potential interaction, on the mouse mucosal response to *C. difficile* infection. Collectively, the acquired data support the following main conclusions: (i) IL-22- and CD160-mediated signalling together account for a significant fraction of the phosphorylated pool of STAT3 in the colons of *C. difficile*-infected mice; and (ii) IL-22 and CD160 play an additive role in mediating both the pro-inflammatory and pro-survival aspects of the mouse mucosal response to *C. difficile* infection.

Anti-IL-22, anti-CD160 and combined anti-IL-22/CD160 treatments all significantly reduced STAT3 phosphorylation in the colons of *C. difficile*-infected mice, hence demonstrating that IL-22 and CD160 are together responsible for a significant fraction of the colonic STAT3 phosphorylation in *C. difficile* infection. However, although anti-IL-22, anti-CD160, and combined anti-IL-22/CD160 treatments led to comparable reductions in STAT3 phosphorylation, anti-CD160 treatment alone had no significant effect on gene expression and anti-IL-22 treatment alone could significantly reduce the expression levels of only two genes. By contrast, the combined use of anti-IL-22 and anti-CD160, at the very same doses that they were used individually, could significantly reduce the expression of 17 genes, including those encoding pro-inflammatory chemokines and cytokines, anti-microbial peptides and pro-survival molecules. Interleukin-22 and CD160 use different signalling pathways to phosphorylate STAT3. In the case of IL-22, STAT3 phosphorylation is through its recruitment to the IL-22 receptor,[42] whereas CD160 uses the nuclear factor-κB-inducing kinase (NIK) to achieve this end.[31] On this basis, we suggest that altering the mucosal gene expression pattern in *C. difficile*-infected mice at the level observed in the CDI + anti-IL-22/CD160 mice would require the concurrent disruption of the pathways used by IL-22 and CD160 for STAT3 phosphorylation, something neither anti-IL-22 nor anti-CD160 can mediate on its own. The availability of CD160$^{-/-}$ mice in the future would allow us to further explore this matter by comparing IL-22R$^{-/-}$, CD160$^{-/-}$ and IL-22R$^{-/-}$/CD160$^{-/-}$ mice infected with *C. difficile*.

Interleukin-22 serves a critical role in promoting inflammation, anti-microbial immunity and tissue repair at mucosal surfaces.[43–47] This is achieved by regulating the expression of genes associated with chemotaxis, inflammation, anti-microbial immunity and tissue repair. STAT3 recruitment and its subsequent phosphorylation are essential for induction of IL-22 through all the pathways characterized so far.[46] Furthermore, the use of STAT3$^{IEC\text{-}KO}$ mice has shown that IL-22-dependent mucosal wound healing is contingent on STAT3 phosphorylation in intestinal epithelial cells.[48] The down-regulation of pro-inflammatory chemokines and cytokines as well as anti-microbial peptides, particularly *Reg3g*,[49] in the colons of CDI + anti-IL-22/CD160 mice, in conjunction with the significant reduction of STAT3 phosphorylation in this setting, provides further evidence for our previous assertion[18] that phosphorylated STAT3, IL-22 and RegIIIγ are an integral part of the host mucosal response to *C. difficile* infection.

Depending on the ligand it binds, the cell types involved and the context of engagement, HVEM can activate co-stimulatory or co-inhibitory signalling pathways.[28–30] The reduced induction of genes for pro-inflammatory chemokines and cytokines, as well as anti-microbial peptides and IL-25, which plays a role in attenuating tissue damage in the gut,[50] in CDI + anti-IL-22/CD160 mice strongly indicates that IL-22 and HVEM-CD160 signalling act in concert to mediate both the pro-inflammatory and pro-survival aspects of the host mucosal response to *C. difficile* infection.

It has been argued that the stereochemistry of LIGHT, BTLA and CD160 binding to HVEM, as well as the *cis* or *trans* nature of the interaction, would predict the behaviour of HVEM in respect of the T-cell response.[51] However, the expression of HVEM and its ligands on a wide range of haematopoietic and non-haematopoietic cells makes this a more challenging task when trying to interpret the outcome of multicellular interactions. This is of particular relevance to the host response in the gut because intestinal epithelial cells, which provide a point of contact for enteric antigens and play a direct role in mucosal immunity, constitutively express HVEM.[21] Expression of HVEM on intestinal epithelial cells may play a crucial role in engaging HVEM ligands on innate and adaptive effector cells in the gut and regulating the direction and intensity of the response. Theoretically, BTLA, LIGHT and CD160 could all engage the intestinal epithelial cell HVEM and act as its functional ligand during *C. difficile* infection. However, a recent study of mouse colonic intraepithelial lymphocytes has shown that they express very low levels of BTLA and LIGHT mRNA but high levels of CD160 mRNA.[31] This leaves CD160 as the most plausible ligand to trigger HVEM signalling on colonic epithelial cells in the course of *C. difficile* infection. The current study shows that, in *C. difficile* infection, CD160 acts in a co-stimulatory capacity. The co-stimulatory role of CD160 is infrequent but documented. *In vitro* findings with human T cells had first raised this possibility.[27] More recent studies have proven CD160's co-stimulatory role in two different *in vivo* models.[31,52] Given that the host response to *C. difficile* infection includes both pro-inflammatory and pro-survival elements, future efforts will need to determine whether the pro-inflammatory and pro-survival effects of HVEM/CD160 signalling in this infection involves one or more subsets of intraepithelial lymphocytes.

While treatment with either anti-IL-22[45] or anti-CD160[31] alone will affect the course of *Citrobacter rodentium* infection in mice, treating *C. difficile*-infected mice with a specified, and previously documented, dose of either anti-IL-22 or anti-CD160 had a limited (anti-IL-22) or non-existent (anti-CD160) significant effect on the gene expression pattern for the evaluated genes, i.e. two genes significantly reduced in the CDI + anti-IL-22 mice and none significantly changed in the CDI + anti-CD160 mice. Although the anti-CD160 clone used in our experiments (clone CNX46-3)[53] is identical to the one used in the *Citrobacter rodentium* infection model,[31] the anti-IL-22 antibody administered in that model (clone 8E11)[45] is different from the one used in our study (clone IL22JOP). Therefore, in the case of anti-IL-22, it could be argued that the difference in outcome between the two infections may simply reflect the distinct effector functions of the two different anti-IL-22 clones. Given that the anti-IL-22 clone used in the current study has been used successfully to affect the severity of inflammation in an *in vivo* model of skin inflammation,[54] its limited effect in *C. difficile*-infected mice cannot be attributed to its lack of biological activity, but it would not be implausible to contend that the dose and duration of its use may not be ideal for an optimal response in the gut. The alternative hypothesis, which we favour, is that the need for the concomitant use of anti-IL-22 and anti-CD160 to affect the gene expression pattern or histopathological outcome in mice infected with *C. difficile* 630 is due to an inherent difference in the biology of *Citrobacter rodentium* and *C. difficile* infections in mice. Our findings that the use of the two antibodies together, at the very same doses that they were used individually, led to a significant reduction in 17 of the 45 evaluated genes and a decrease in neutrophil influx to the site of infection, provides strong empirical support for this hypothesis.

As discussed in detail in our previous work,[18] the genes induced in response to *C. difficile* infection fall into three broad categories: first, chemokines, which play a pivotal role in recruiting effector cells of the innate immune system to the site of infection; second, pro-inflammatory cytokines, which mediate inflammatory effector functions at the site of infection and in turn contribute to the up-regulation of chemokines such as *Cxcl1*, *Ccl2*, *Cxcl9* and *Cxcl10*; and third, *Il22* and anti-microbial peptides, which mediate the host's efforts to maintain epithelial integrity. The optimal outcome of these gene up-regulations is to contain the *C. difficile*-induced inflammation and to minimize mucosal damage by promoting epithelial homeostasis.[18,55]

The CDI + anti-IL-22/CD160 mice show a simultaneous and significant reduction in the expression of a number of chemokines, pro-inflammatory cytokines and anti-microbial peptides. This could arguably reflect the host's effort to curtail the extent of host-mediated immunopathology. Under this scenario, the lower intensity of inflammation would incur less host-mediated damage at the site of infection, therefore decreasing the required level of homeostatic activity for restoring epithelial integrity. In this study, the observed early histopathological and flow cytometric manifestation of anti-IL-22/CD160 treatment in *C. difficile*-infected mice is anti-inflammatory. Based on the prolonged course of infection with *C. difficile* 630,[33] we believe that the histopathological epithelial manifestation of anti-IL-22/CD160's effect on expression levels of *Reg3g*, *Il25*, etc., as well as its potential effect on bacterial load, would require a longer course of infection and antibody treatment than was undertaken in the current study; this will be the first focus of our future efforts.

Taking our cue from the work done on sustaining eIF2α phosphorylation in prion-induced neurodegeneration,[56] we had argued that manipulating common biochemical pathways, rather than disease- and pathogen-specific approaches, could potentially be of therapeutic benefit across a spectrum of conditions with analogous and/or shared pathophysiologies.[18] Our current findings with the combined use of anti-IL-22/CD160 in *C. difficile* infection, together with the report on the contribution of HVEM/CD160 to host defence against *Citrobacter rodentium* infection in the gut and *Streptococcus pneumoniae* infection in the lung,[31] gives further credence to this concept in the context of infection and could serve as a point of departure for a new approach for affecting an infection's outcome.

Acknowledgements

This work was supported by NIH grants U19 AI090871 (VBY and GBH), and P30 DK034933 (VBY and GBH).

Disclosure

The authors declare no commercial or financial conflict of interest.

References

1 Hall I, O'Toole E. Intestinal flora in newborn infants with description of a new pathogenic anaerobe. *Am J Dis Child* 1935; **49**:390–402.
2 Kelly CP, LaMont JT. *Clostridium difficile* infection. *Annu Rev Med* 1998; **49**:375–90.
3 Rupnik M, Wilcox MH, Gerding DN. *Clostridium difficile* infection: new developments in epidemiology and pathogenesis. *Nat Rev Microbiol* 2009; **7**:526–36.
4 Britton RA, Young VB. Interaction between the intestinal microbiota and host in *Clostridium difficile* colonization resistance. *Trends Microbiol* 2012; **20**:313–9.
5 Eyre DW, Cule ML, Wilson DJ *et al.* Diverse sources of *C. difficile* infection identified on whole-genome sequencing. *N Engl J Med* 2013; **369**:1195–205.
6 Just I, Selzer J, von Eichel-Streiber C, Aktories K. The low molecular mass GTP-binding protein Rho is affected by toxin A from *Clostridium difficile*. *J Clin Invest* 1995; **95**:1026–31.
7 Just I, Selzer J, Wilm M, von Eichel-Streiber C, Mann M, Aktories K. Glucosylation of Rho proteins by *Clostridium difficile* toxin B. *Nature* 1995; **375**:500–3.
8 Hecht G, Pothoulakis C, LaMont JT, Madara JL. *Clostridium difficile* toxin A perturbs cytoskeletal structure and tight junction permeability of cultured human intestinal epithelial monolayers. *J Clin Invest* 1988; **82**:1516–24.

9 Hecht G, Koutsouris A, Pothoulakis C, LaMont JT, Madara JL. *Clostridium difficile* toxin B disrupts the barrier function of T84 monolayers. *Gastroenterology* 1992; **102**:416–23.

10 Pothoulakis C, Lamont JT. Microbes and microbial toxins: paradigms for microbial–mucosal interactions II. The integrated response of the intestine to *Clostridium difficile* toxins. *Am J Physiol Gastrointest Liver Physiol* 2001; **280**:G178–83.

11 Johnson S, Gerding DN. *Clostridium difficile*-associated diarrhea. *Clin Infect Dis* 1998; **26**:1027–34; quiz 35-6.

12 Lawley TD, Clare S, Walker AW *et al.* Antibiotic treatment of *Clostridium difficile* carrier mice triggers a supershedder state, spore-mediated transmission, and severe disease in immunocompromised hosts. *Infect Immun* 2009; **77**:3661–9.

13 Ryan A, Lynch M, Smith SM *et al.* A role for TLR4 in *Clostridium difficile* infection and the recognition of surface layer proteins. *PLoS Pathog* 2011; **7**:e1002076.

14 Hasegawa M, Yamazaki T, Kamada N, Tawaratsumida K, Kim YG, Nunez G, Inohara N. Nucleotide-binding oligomerization domain 1 mediates recognition of *Clostridium difficile* and induces neutrophil recruitment and protection against the pathogen. *J Immunol* 2011; **186**:4872–80.

15 Hasegawa M, Kamada N, Jiao Y, Liu MZ, Nunez G, Inohara N. Protective role of commensals against *Clostridium difficile* infection via an IL-1β-mediated positive-feedback loop. *J Immunol* 2012; **189**:3085–91.

16 Jarchum I, Liu M, Lipuma L, Pamer EG. Toll-like receptor 5 stimulation protects mice from acute *Clostridium difficile* colitis. *Infect Immun* 2011; **79**:1498–503.

17 Jarchum I, Liu M, Shi C, Equinda M, Pamer EG. Critical role for MyD88-mediated neutrophil recruitment during *C. difficile* colitis. *Infect Immun* 2012; **80**:2989–96.

18 Sadighi Akha AA, Theriot CM, Erb-Downward JR *et al.* Acute infection of mice with *Clostridium difficile* leads to eIF2α phosphorylation and pro-survival signalling as part of the mucosal inflammatory response. *Immunology* 2013; **140**:111–22.

19 Montgomery RI, Warner MS, Lum BJ, Spear PG. Herpes simplex virus-1 entry into cells mediated by a novel member of the TNF/NGF receptor family. *Cell* 1996; **87**:427–36.

20 Anderson CA, Boucher G, Lees CW *et al.* Meta-analysis identifies 29 additional ulcerative colitis risk loci, increasing the number of confirmed associations to 47. *Nat Genet* 2011; **43**:246–52.

21 Steinberg MW, Turovskaya O, Shaikh RB *et al.* A crucial role for HVEM and BTLA in preventing intestinal inflammation. *J Exp Med* 2008; **205**:1463–76.

22 Schaer C, Hiltbrunner S, Ernst B, Mueller C, Kurrer M, Kopf M, Harris NL. HVEM signalling promotes colitis. *PLoS ONE* 2011; **6**:e18495.

23 Whitbeck JC, Peng C, Lou H *et al.* Glycoprotein D of herpes simplex virus (HSV) binds directly to HVEM, a member of the tumor necrosis factor receptor superfamily and a mediator of HSV entry. *J Virol* 1997; **71**:6083–93.

24 Mauri DN, Ebner R, Montgomery RI *et al.* LIGHT, a new member of the TNF superfamily, and lymphotoxin α are ligands for herpesvirus entry mediator. *Immunity* 1998; **8**:21–30.

25 Sedy JR, Gavrieli M, Potter KG *et al.* B and T lymphocyte attenuator regulates T cell activation through interaction with herpesvirus entry mediator. *Nat Immunol* 2005; **6**:90–8.

26 Cai G, Anumanthan A, Brown JA, Greenfield EA, Zhu B, Freeman GJ. CD160 inhibits activation of human CD4$^+$ T cells through interaction with herpesvirus entry mediator. *Nat Immunol* 2008; **9**:176–85.

27 Cheung TC, Steinberg MW, Oborne LM *et al.* Unconventional ligand activation of herpesvirus entry mediator signals cell survival. *Proc Natl Acad Sci USA* 2009; **106**:6244–9.

28 Kaye J. CD160 and BTLA: LIGHTs out for CD4$^+$ T cells. *Nat Immunol* 2008; **9**:122–4.

29 Cai G, Freeman GJ. The CD160, BTLA, LIGHT/HVEM pathway: a bidirectional switch regulating T-cell activation. *Immunol Rev* 2009; **229**:244–58.

30 Ware CF, Sedy JR. TNF Superfamily Networks: bidirectional and interference pathways of the herpesvirus entry mediator (TNFSF14). *Curr Opin Immunol* 2011; **23**:627–31.

31 Shui JW, Larange A, Kim G, Vela JL, Zahner S, Cheroutre H, Kronenberg M. HVEM signalling at mucosal barriers provides host defence against pathogenic bacteria. *Nature* 2012; **488**:222–5.

32 Perez J, Springthorpe VS, Sattar SA. Clospore: a liquid medium for producing high titers of semi-purified spores of *Clostridium difficile*. *J AOAC Int* 2011; **94**:618–26.

33 Theriot CM, Koumpouras CC, Carlson PE, Bergin II, Aronoff DM, Young VB. Cefoperazone-treated mice as an experimental platform to assess differential virulence of *Clostridium difficile* strains. *Gut Microbes* 2011; **2**:326–34.

34 Antonopoulos DA, Huse SM, Morrison HG, Schmidt TM, Sogin ML, Young VB. Reproducible community dynamics of the gastrointestinal microbiota following antibiotic perturbation. *Infect Immun* 2009; **77**:2367–75.

35 Reeves AE, Theriot CM, Bergin IL, Huffnagle GB, Schloss PD, Young VB. The interplay between microbiome dynamics and pathogen dynamics in a murine model of *Clostridium difficile* infection. *Gut Microbes* 2011; **2**:145–58.

36 Schmittgen TD, Livak KJ. Analyzing real-time PCR data by the comparative C(T) method. *Nat Protoc* 2008; **3**:1101–8.

37 Reeves AE, Koenigsknecht MJ, Bergin IL, Young VB. Suppression of *Clostridium difficile* in the gastrointestinal tracts of germfree mice inoculated with a murine isolate from the family Lachnospiraceae. *Infect Immun* 2012; **80**:3786–94.

38 Sadighi Akha AA, Harper JM, Salmon AB, Schroeder BA, Tyra HM, Rutkowski DT, Miller RA. Heightened induction of proapoptotic signals in response to endoplasmic reticulum stress in primary fibroblasts from a mouse model of longevity. *J Biol Chem* 2011; **286**:30344–51.

39 Vandesompele J, De Preter K, Pattyn F, Poppe B, Van Roy N, De Paepe A, Speleman F. Accurate normalization of real-time quantitative RT-PCR data by geometric averaging of multiple internal control genes. *Genome Biol* 2002; **3**:RESEARCH0034.

40 Tusher VG, Tibshirani R, Chu G. Significance analysis of microarrays applied to the ionizing radiation response. *Proc Natl Acad Sci USA* 2001; **98**:5116–21.

41 Krzywinski M, Altman N. Points of significance: comparing samples – part II. *Nat Methods* 2014; **11**:355–6.

42 Dumoutier L, de Meester C, Tavernier J, Renauld JC. New activation modus of STAT3: a tyrosine-less region of the interleukin-22 receptor recruits STAT3 by interacting with its coiled-coil domain. *J Biol Chem* 2009; **284**:26377–84.

43 Wolk K, Kunz S, Witte E, Friedrich M, Asadullah K, Sabat R. IL-22 increases the innate immunity of tissues. *Immunity* 2004; **21**:241–54.

44 Liang SC, Tan XY, Luxenberg DP, Karim R, Dunussi-Joannopoulos K, Collins M, Fouser LA. Interleukin (IL)-22 and IL-17 are coexpressed by Th17 cells and cooperatively enhance expression of antimicrobial peptides. *J Exp Med* 2006; **203**:2271–9.

45 Zheng Y, Valdez PA, Danilenko DM *et al.* Interleukin-22 mediates early host defense against attaching and effacing bacterial pathogens. *Nat Med* 2008; **14**:282–9.

46 Ouyang W, Rutz S, Crellin NK, Valdez PA, Hymowitz SG. Regulation and functions of the IL-10 family of cytokines in inflammation and disease. *Annu Rev Immunol* 2011; **29**:71–109.

47 Sonnenberg GF, Fouser LA, Artis D. Border patrol: regulation of immunity, inflammation and tissue homeostasis at barrier surfaces by IL-22. *Nat Immunol* 2011; **12**:383–90.

48 Pickert G, Neufert C, Leppkes M *et al.* STAT3 links IL-22 signaling in intestinal epithelial cells to mucosal wound healing. *J Exp Med* 2009; **206**:1465–72.

49 Vaishnava S, Yamamoto M, Severson KM *et al.* The antibacterial lectin RegIIIγ promotes the spatial segregation of microbiota and host in the intestine. *Science* 2011; **334**:255–8.

50 Franze E, Rizzo A, Caruso R, Pallone F, Monteleone G. Interleukin-25 negatively controls pathogenic responses in the gut. *Inflamm Allergy Drug Targets* 2011; **10**:187–91.

51 Steinberg MW, Cheung TC, Ware CF. The signaling networks of the herpesvirus entry mediator (TNFRSF14) in immune regulation. *Immunol Rev* 2011; **244**:169–87.

52 D'Addio F, Ueno T, Clarkson M *et al.* CD160Ig fusion protein targets a novel costimulatory pathway and prolongs allograft survival. *PLoS ONE* 2013; **8**:e60391.

53 Maeda M, Carpenito C, Russell RC *et al.* Murine CD160, Ig-like receptor on NK cells and NKT cells, recognizes classical and nonclassical MHC class I and regulates NK cell activation. *J Immunol* 2005; **175**:4426–32.

54 Park SY, Gupta D, Hurwich R, Kim CH, Dziarski R. Peptidoglycan recognition protein Pglyrp2 protects mice from psoriasis-like skin inflammation by promoting regulatory T cells and limiting Th17 responses. *J Immunol* 2011; **187**:5813–23.

55 Buffie CG, Pamer EG. Microbiota-mediated colonization resistance against intestinal pathogens. *Nat Rev Immunol* 2013; **13**:790–801.

56 Moreno JA, Radford H, Peretti D *et al.* Sustained translational repression by eIF2α-P mediates prion neurodegeneration. *Nature* 2012; **485**:507–11.